Transcriptome profiling of laser-captured germ cells and functional characterization of zbtb40 during MT-induced spermatogenesis in orange-spotted grouper (Epinephelus coioides)

Xiaochun Liu (lsslxc@mail.sysu.edu.cn)
Sun Yat-Sen University
Xi Wu
Sun Yat-Sen University
Yang Yang
Sun Yat-Sen University
Chaoyue Zhong
Sun Yat-Sen University
Yin Guo
Sun Yat-Sen University
Shuisheng Li
Sun Yat-Sen University
Haoran Lin
Sun Yat-Sen University

Research article

Keywords: Spermatogenesis, transcriptome, laser capture microdissection, grouper, zbtb40

Posted Date: July 12th, 2019

DOI: https://doi.org/10.21203/rs.2.11289/v1

Version of Record: A version of this preprint was published on January 23rd, 2020. See the published version at https://doi.org/10.1186/s12864-020-6477-4.

Abstract

Background: Spermatogenesis is an intricate process regulated by a finely organized network. The orange-spotted grouper (Epinephelus coioides) is a protogynous hermaphroditic fish, but the process of its spermatogenesis is not well-understood. In the present study, transcriptome sequencing of the male germ cells from orange-spotted grouper was performed to explore the molecular mechanisms underlying spermatogenesis. Results: In this study, the orange-spotted grouper was induced to change sex from female to male by 17alpha-methyltestosterone implantation. During the artificial spermatogenesis, different cell types from cysts containing spermatogonia, spermatocytes, spermatids, and spermatozoa were isolated by laser capture microdissection. Subsequently, transcriptomic analysis for the isolated cells were performed. A series of genes was used to verify and investigate the expression patterns in spermatogenesis. Furthermore, we also analyzed the expression of the same set of genes involved with steroid metabolism and sex throughout spermatogenesis (early-mid, late, and maturing stages) in the orange-spotted grouper. Several generally female-related genes took significantly changes in sex reversal hinted that the female-related genes in previously recognized may also play vital roles in spermatogenesis and sex reversal. In the transcriptomic data, we focused on zbtb family genes, which may be related to the process of spermatogenesis. Their expression patterns and cellular localization were examined, and the location of Eczbtb40 in different gonadal stages was investigated. We found that Eczbtb40 was expressed throughout spermatogenesis. These preliminary findings suggest that Eczbtb40 is highly conserved during vertebrate evolution and plays roles in spermatogenesis. Besides, the expression of Eczbtb40 and Eccyp17a1a overlapped in male germ cells, especially spermatogonium and spermatocyte, which suggested that Eczbtb40 might interact with Eccyp17a1a participant in spermatogenesis and sex reversal. Conclusions: The present study first depicted RNA sequencing of the male germ cells from orange-spotted grouper, and identified many important functional genes and pathways involved in spermatogenesis. The Eczbtb40 gene was subjected to molecular characterization and expression pattern analysis. These results will contribute to future studies of the molecular mechanism of spermatogenesis and sex reversal.

Abstract

Background: Spermatogenesis is an intricate process regulated by a finely organized network. The orange-spotted grouper (*Epinephelus coioides*) is a protogynous hermaphroditic fish, but the process of its spermatogenesis is not well-understood. In the present study, transcriptome sequencing of the male germ cells from orange-spotted grouper was performed to explore the molecular mechanisms underlying spermatogenesis.

Results: In this study, the orange-spotted grouper was induced to change sex from female to male by 17alpha-methyltestosterone implantation. During the artificial spermatogenesis, different cell types from cysts containing spermatogonia, spermatocytes, spermatids, and spermatozoa were isolated by laser capture microdissection. Subsequently, transcriptomic analysis for the isolated cells were performed. A series of genes was used to verify and investigate the expression patterns in spermatogenesis.

Furthermore, we also analyzed the expression of the same set of genes involved with steroid metabolism and sex throughout spermatogenesis (early-mid, late, and maturing stages) in the orange-spotted grouper. Several generally female-related genes took significantly changes in sex reversal hinted that the female-related genes in previously recognized may also play vital roles in spermatogenesis and sex reversal. In the transcriptomic data, we focused on *zbtb* family genes, which may be related to the process of spermatogenesis. Their expression patterns and cellular localization were examined, and the location of *Eczbtb40* in different gonadal stages was investigated. We found that *Eczbtb40* wasexpressed throughout spermatogenesis.These preliminary findings suggest that *Eczbtb40* is highly conserved during vertebrate evolution and plays roles in spermatogenesis. Besides, the expression of *Eczbtb40* and *Eccyp17a1a* overlapped in male germ cells, especially spermatogonium and spermatocyte, which suggested that *Eczbtb40* might interact with *Eccyp17a1a* participant in spermatogenesis and sex reversal.

Conclusions: The present study first depicted RNA sequencing of the male germ cells from orange-spotted grouper, and identified many important functional genes and pathways involved in spermatogenesis. The *Eczbtb40* gene was subjected to molecular characterization and expression pattern analysis. These results will contribute to future studies of the molecular mechanism of spermatogenesis and sex reversal.

Keywords: Spermatogenesis, transcriptome, laser capture microdissection, grouper, *zbtb40*

Background

Transcriptome sequencing is a technology to catalogue all species of transcript, determine the transcriptional structure of genes, and quantify the expression of every transcript under different conditions [1]. Comparison of transcriptomes can provide both quantitative and qualitative information on genetic activity [2]. When gross tissue extracts are used as an mRNA source, tissue heterogeneity confounds assigning expressed genes to different cell populations [3]. Although some *in situ* technologies, such as *in situ* hybridization or immunohistochemistry, could confirm the spatial expression of specific gene, when numerous messages need to be examined, these technologies might not always be possible and is laborious and time consuming [4]. Hence, many researchers have tried to develop microdissection protocols to yield mRNA with sufficient quality for the subsequent transcriptomic analysis. Because of the speed, precision, and versatility, laser capture microdissection (LCM) was applied in omics , including transcriptome [5, 6] and proteome [7].

LCM is a technology first developed in the late 1990s for obtaining pure populations of targeted cells from specific microscopic regions of tissue sections for subsequent analysis. LCM is a microscope-based technology involving sampling, sample embedding, cryosection, visualization of the target cells, adjustment of the cutting parameters, selecting the target areas, and collection of dissected cells into a tube [8]. The technology was first applied to study gene expression in human cancer cells and gene expression during spermatogenesis in rodents [9-11]. Subsequently, many researcher used LCM to acquire

different male germ cells during spermatogenesis for detecting the expression of important genes in many other species, including European sea bass [12], zebrafish [13-15], and African catfish [16].

We first used LCM to obtain male germ cells from different developmental stages induced by 17alpha-methyltestosterone (MT) to profile the natural process of spermatogenesis in orange-spotted grouper (*Epinephelus coioides*). Grouper is a protogynous hermaphroditic fish underlying sex change from female to male in the life history [17]. It has been considered as a good model for the study of sex differentiation, ovarian development, and sex reversal. Because of lack of male fish, few studies of spermatogenesis has been conducted out in orange-spotted grouper. To profile the process of spermatogenesis in grouper, the LCM protocol was optimized to obtain the four germ cell types from male grouper induced by MT implantation, including spermatogonia (SG), spermatocytes (SC), spermatids (ST), and spermatozoa (SZ).

Spermatogenesis is a developmental process in which diploid male germ cells transform into haploid functional male gametes in a tight spatial and temporal organization. Spermatogonia develop into primary spermatocytes, which becomes haploid spermatids through two meiotic divisions without DNA replication, finally transforming into mature spermatozoa. These processes are achieved by a complex network involving many genes, the germ cells themselves, and several somatic cell types (i.e. Sertoli cells and Leydig cells) [18]. The structural and functional aspects of spermatogenesis are highly conserved among the vertebrates [19]. The release of gonadotropic hormones (follicle-stimulating hormone, luteinizing hormone, growth hormone) released from pituitary stimulate the testis to produce the androgens that initiate spermatogenesis [19]. Hormonal control is a complicated network affected by many stage-specific and cell-specific factors [13, 20].

Previously, quantifying specific genes is difficult because the complex testis structure contains various cell types. Some approaches can be used to quantify and localize unique genes, including *in situ* hybridization [21, 22], serial analysis of gene expression (SAGE) [23, 24], and *in vitro* culture of the specific cell population [25]. However, these methods exist some problems to overcome, like the time it takes, the difficulty of the approach itself, etc. Subsequently, researchers have focused on LCM and established an optimized method to obtain specific cell types for studying spermatogenesis. Nevertheless, it is still difficult to isolate the somatic cells around the germ cells to mirror the intricate relationship between somatic cells and different male germ cells during spermatogenesis.

So in our study, transcriptome sequencing was conducted combining LCM to obtain specific cell type to explore the spermatogenesis induced by 17alpha-methyltestosterone (MT) in order to reveal the natural spermatogenesis in a new aspect. Transcriptomic analysis was performed with the goal of revealing the differential gene expression and regulatory networks and *zbtb* genes came into our sight. Zinc finger and BTB (broad complex, Tramtrack, and Bric-à-brac) (ZBTB) proteins are an evolutionarily conserved family of transcription factors.

Approximately 60 ZBTB proteins has been identified involving in diverse functions including development, differentiation, and oncogenesis [26-28]. In recent years, ZBTB16 was found to play an

essential role in spermatogenesis by controlling the self-renew and differentiation of spermatogonium [29-32]. In the transcriptome data, we found that several *zbtb* family genes was differently expressed. Further, the *zbtb* family genes were identified and their expression were investigated during the process of sex reversal and spermatogenesis, and the expression pattern and potential function of *Eczbtb40* were determined in spermatogenesis.

Results

D evelopmental stages of gonads during MT-induced sex reversal

As shown in the Fig. 1, fish oocytes in the sham group remained in the primary-growth stage throughout the experimental period. In contrast, the fish in MT-implanted group underwent sex reversion from female to male. In the first week of MT implantation, the gonads were characterized by degeneration of oocytes and simultaneous proliferation of spermatogenic cysts (Week 1; Fig. 1C). At two weeks after MT implantation, the gonads entered into the intermediate transitional stage filled with SG and SC and numerous oocytes (Week 2; Fig. 1E). At three weeks after MT implantation, the gonads transformed into functional testis, comprised mostly of ST, a small number of SZ, and a few oocytes (Week 3; Fig. 1G).

Capture of target cells

The morphology of SG, SC, and ST were characterized by hematoxylin and eosin (H&E) (Fig.2A) and cryosection staining (Fig.2B). SZ was obtained from the functional testis. During spermatogonia differentiation, the density of heterochromatin reached a the maximum in type B late spermatogonia [33]. When spermatid changed into sperm, the DNA was maximally compacted [18]. Thus, the sizes of the four types of male germ cells decreased (SG > SC > ST > SZ) and staining of the cell nucleus became darker. Four different male germ cells were detected in tissue slices based on these characteristics.

Validation of sample specificity

Six genes were used to examine the purity of the LCM-derived RNA samples (Fig.3A). *ef1a* is a reference gene and commonly used as an internal control for gene expression analysis. Its expression was detected in all four types of male germ cells at similar levels. Vasa is a germ cell marker [34] whose expression was also found in the four cell types. *slbp2* was specifically expressed in the oocyte of orange-spotted grouper [35], while no expression was detectedin any male germ cells except for in the positive control (the gonad with mainly primary-growth stage oocytes). *dmrt1* was specifically expressed in the spermatogenic cells of orange-spotted grouper [36]. Here, *dmrt1* was only expressed in SG and SC with no expression in the positive or negative control.

Quality of transcriptomic data

Four cDNA libraries (SG, SC, ST, and SZ) were constructed with the respective RNA extracted from different male germ cell types of orange-spotted grouper by LCM. The cDNA libraries were sequenced on an Illumina Hiseq 2000 platform (San Diego, CA, USA). A total of 25,304, 890 raw reads were obtained,

and a total of 244, 984, 338 clean reads were produced after removing low-quality reads and adapter sequences (Table 1). The average Q20 and Q30 values were 95.74% and 90.57% respectively, and the content of GC was 44.08–47.47%, reflecting the accuracy of the transcriptomic data.

Differentially expressed genes (DEGs) among the four cell types（SG, SC, ST, and SC）

Fragments per kilobase million (FPKMs) were used to quantify the gene expression levels. The FPKM values of each gene in the four cell types were compared respectively (Additional file 1). There were 16,406 up-regulated genes and 11,054 down-regulated genes in SG compared to SC. A total of 15,845 up-regulated genes and 6,895 down-regulated genes were identified in SC to ST. The STs had 8,320 up-regulated genes and 15,797 down-regulated genes compared to SZ. And SG had 22,599 up-regulated genes and 7,399 down-regulated genes relative to STs. There were 14,624 up-regulated genes and 12,413 down-regulated genes in SC compared to SZ. Among the four cell types, 4,483 DEGs were detected and analyzed.

GO and KEGG enrichment of DEGs

In the biological process and molecular function categories of the 4483 DEGs, cellular process (GO: 0009987) and binding (GO: 0005488) were the most enriched GO terms (Fig. S1). And the top 20 pathways were listed from KEGG enrichment (Fig. 4A). Among them, differentiation pathways, signal pathways, and metabolism pathways, which may play crucial roles during spermatogenesis, were observed.

Expression of functional genes putatively associated with sex differentiation and steroid metabolism

From the transcriptomic data, the expression of 20 genes putatively related to sex differentiation and steroid metabolism were analyzed (Fig.5 and 6). Eight of the sex differentiation genes (*sox11a*, *nr0b1*, *era*, *erb*, *wnt9*, *gdf9*, and *bmp15*) and 13 of the short-chain dehydrogenases/reductases (SDR) genes (*cyp17a1*, *3hd*, *sdr12*, *sdr11*, *p5cdh*, *cyp3a40*, and *sdr13*) which are involved in steroid metabolism were expressed in different cell types with FPKM values ranging from 2.62 to 604.7. Most of these genes showed peak expression in SG and SZ (Fig. 4 B).

RT-PCR validation of gene expression inferred from transcriptomic data

RT-PCR was conducted to validate the expression patterns of 13 genes predicted to be involved with sex differentiation and steroid metabolism (asterisk-marked genes in Fig. 4) and deduced from the transcriptomic data. As shown in Figs. 5 and 6, all of these genes were significantly changed in the process of sex reversal, which was mostly consistent with the transcriptomic data. These results indicate that the expressional analysis based on RNA-seq data was credible in the present study.

Molecular cloning and sequence analysis of *Eczbtb40*

Among the 4438 DEGs in four cell types, several *zbtb* genes including *zbtb1*, *zbtb22*, *zbtb40*, and *zbtb44* attracted our attention. ZBTB family proteins are transcription factors that participate in various important functions. It's reported that *zbtb16* (*plzf*) played an important role in the self-renewal and differentiation of the undifferentiated spermatogonia [29]. Therefore, whether the *zbtb* genes regulate in spermatogenesis of orange-spotted grouper was examined. We studied the expression of the *zbtb* genes (*zbtb1*, *zbtb22*, *zbtb40*, and *zbtb44*) to determine their functions in spermatogenesis (Fig. S3). After further verification, *Eczbtb40* was came into our sight, and then deeply functions and expression patterns were exploited.

The open reading frame (ORF) of *zbtb40* was cloned from the testis of orange-spotted grouper, which were denominated as *Eczbtb40*. As shown in Fig. S2, *Eczbtb40* consisted of a 2400-base pair ORF encoding a peptide of 799 amid acids. Amino acid sequence alignment and comparison analysis indicated that *zbtb40* contains a conserved domain (Fig. S4). A phylogenetic tree was constructed based on amino acid sequences of the known *zbtb40* genes (Fig. 7A). On the tree, *Epinephelus coioides zbtb40* was clustered together with *Larimichys crocea zbtb40*. The *zbtb40*s contains variously conserved sites in all selected species, among them the top ten motif sites were showed (Fig. 7B). The DNA sequence of each motif site was displayed in Tab. S1.

Tissue distribution of *Eczbtb40*

Expression of *Eczbtb40* was examined in eight tissues by semi-quantitative PCR. The results revealed very high *Eczbtb40* expression in the testis, heart, and pituitary and weak expression in whole brain, head kidney, liver, and ovary (Fig.3B).

Expression profiles of *Eczbtb40* in gonads during MT-induced sex reversal

The expression pattern of the *Eczbtb40* during the MT-induced sex reversal process was investigated. *Eczbtb40* expression showed no significant difference from the control groups (Fig. 6H). The mRNA levels in MT-treated fish were significantly higher than those in the control group in the second weeks.

In situ localization of Ec*zbtb*40 in gonads during sex reversal

At the early stage of sex reversal, there were still a large number of primary-growth stage oocytes which wasn't detected the expression of *Eczbtb40*mRNA (Fig. 8B). At the middle stage of sex reversion, many spermatogonia and spermatocytes emerged, showing *Eczbtb40* mRNA expression (Fig. 8C). At the late stage of sex reversal, there were few oocytes in the gonad and *Eczbtb40* was abundantlyexpressed in SG, SC, ST, and SC (Fig. 8D). In comparison, no signal was detected in the ovary from the control group and sham group (Fig. 8A).

Co-localization of *Eczbtb40* and *Eccyp17a1* in gonads during MT-induced sex reversal

Using the JASPAR CORE 2018 database of transcription factor DNA-binding sites, a match was found between an *Eczbtb40* MEME-generated consensus sequence and the *Eccyp17a1* consensus DNA binding

site (Tab. S1). The subcellular localization and co-localization of *Eczbtb40* and *Eccyp17a* in gonads cells were examined during MT-induced sex reversal by fluorescence *in situ* hybridization under a confocal microscope (Fig. 9). In ovary, *Eczbtb40* showed little signal, while *Eccyp17a1* signals were clearly present in the cytoplasm of primary growth stage oocyte (Fig. 9A-D). In testis, the signals of *Eczbtb40* in the cytoplasm of SG and SC were overlapped with the *Eccyp17a1* signals (Fig. 9E-H). Both *Eczbtb40* and *Eccyp17a1* showed weak signals in ST and SZ. The signals were observed nearly exclusively in the cytoplasm but were barely detectable in the nucleus.

Discussion

In present study, transcriptome analysis was used to profile the process of spermatogenesis based on the LCM technology. A large number of differently expressed genes and signal pathways related to spermatogenesis were identified in this study.

Quality and purity of the LCM-derived RNA

The whole process of LCM must produce a sufficient amount of RNA with high quality to ensure the reliability of the transcriptome results. Single-cell LCM requires a long microdissection period and the yield of RNA is limited. In this study, we modified a previous protocol [37] to handle slides and tissues, samples staining and capture the cells for preserving the RNA integrity throughout microdissection.

To verify the purity of the four target cells, several cell markers were detected. The expression of *ef1a* indicated the homogeneity of concentration in four cell types. *Vasa*, a germ cell marker [38], is required for proper germ cells development. Its expression levels were decreased gradually with the process spermatogenesis which is consistent with the expression pattern of *vasa* in the male germ cells of the gibel carp [38] and brown-marbled grouper [34]. As an oocyte-specific marker [35, 39], *slbp2* was used to distinguish the female germ cell and male germ cell. The non-expression of *slbp2* in four cell types indicated that target cells didn't contaminate by female germ cells. *dmrt1* was used as a spermatogenic cell marker [40] and is only expressed in SG and SC but not in ST and SZ in orange-spotted grouper. Based on the expression of these cell markers, the four target cells were considered to be pure. The quality and purity of the LCM-derived RNA met the criterion for constructing the single cell transcriptome library after a series of detection.

Transcriptome overview of spermatogenesis in orange-spotted grouper

In the present study, male germ cells during MT-induced spermatogenesis were used to explore the natural spermatogenesis and profile the expression patterns of genes related to the sex differentiation and steroid metabolism. Omics resources with orange-spotted grouper are extremely limited so far. The transcriptome sequencing of spermatogenesis can generate a wealth of data, which is useful for further understanding the basic biological mechanisms of spermatogenesis in orange-spotted grouper. KEGG pathway analysis revealed that some biological pathways putatively involved in gonadal development were obtained, including osteoclast differentiation, apoptosis, and retinol metabolism, which is similar to

the case in sea bass [12] and Senegalese sole [41] . In addition, the present data showed that 35 DEGs were enriched to Wnt signaling pathway, 5 DEGs were enriched to steroid biosynthesis, 25 DEGs were enriched to Estrogen signaling pathway, 25 DEGs were enriched to cell cycle, 24 DEGs were enriched to oocyte meiosis and 7 DEGs were enriched to ovarian steroidogenesis. These pathways should be evaluated to explore their roles in sex reversal and spermatogenesis.

The orphan nuclear receptor 0 B1 (Nr0B1) is related to many important functions including sex determination, embryonic development, neural differentiation and gonadal steroidogenesis in mammals [42, 43]. Nr0B1 homologues have been identified in several types of teleost such as zebrafish [44], Nile tilapia [45], European sea bass [46], rice-field eel [47], and scallop [48]. The expression pattern of *nr0b1* in rice-field eel revealed that it may be involved in the maintenance of testis function [47]. And *nr0b1* was mainly located in spermatogonia and spermatocytes of testis in scallop, indicating a potential role in spermatogenesis [48]. The significant decrease in *nr0b1* at one week after MT-implantation (Fig. 5A) also verified its potential effect in the spermatogenesis of orange-spotted grouper. Estrogen receptors (ERs) are composed of two related subtypes, ERα and ERβ, which play roles in sex development and reproduction [49-51]. It was reported that the transcriptional activity of liganded ERs is inhibited by Nr0B1 possibly affecting the recruitment of corepressors [52]. ERα and ERβ were significantly increased after MT-implantation, likely because *nr0b1* was decreased inorange-spotted grouper (Fig. 5B, C). This suggested that estrogen and ERs are important in both male and female.

Wnt genes encode a large family of secreted factors with diverse roles in governing cell fate, proliferation, migration, polarity, and death [53]. Although few studies have evaluated the role of *wnt9* in testis, the significant increase in *wnt9* during sex reversal revealed its potential role in spermatogenesis (Fig. 5D). A previous study showed that the oocyte-secreted growth differentiation factor (GDF) 9 and bone morphogenetic protein 15 (BMP15) regulate the growth, differentiation, and function of granulosa and thecal cells during follicular development in oocyte development, ovulation, fertilization, and embryonic competence [54]. An increasing number of studies has focused on the function of GDF9 in the testis. GDF9 mRNA in the testis of mouse, rat, and human is specifically detected in two of the germ cell types: large spermatocytes, and round spermatids [55]. Recombinant GDF9 was reported to disrupt the inter-Sertoli tight junction permeability barrier *in vitro* [56], suggesting that *gdf9* regulates spermatogenesis *in vivo*. Similarly, there are several reports of the transcript or protein of BMP15 in testis and its role in testicular functions, indicating that *bmp15* functions in the testis as in the ovary [57, 58]. In our study, the significant changes in *gdf9* and *bmp15* adequately indicate their potential roles in the sex reversal or spermatogenesis of orange-spotted grouper. Overall, the significantly changes in several generally female-related genes indicate that female-related genes may also play vital roles in spermatogenesis and sex reversal. These genes should be further explored in the context of spermatogenesis and sex reversal.

Possible function of *Eczbtb40* in spermatogenesis

Few studies have examined the function of ZBTB40. In our data, *Eczbtb40* isonly expressed in male germ cells and is important in the process of sex reversal. Gender-specific expression of *Eczbtb40* indicatedthat

it may participate in the process of spermatogenesis, too. The predicted result by software suggests that transcription factor *Eczbtb40* may regulate *Eccyp17a1*. Hence, fluorescence *in situ* hybridization for the newly identified *Eczbtb40* was co-localized with *Eccyp17a1* in SG and SC during spermatogenesis further. *cyp17a1* (steroid 17-alpha-hydroxylase/17, 20 lyase) catalyzes both the 17-alpha-hydroxylation and the 17, 20-lyase reaction. In *cyp17a1*-deficient zebrafish, male-typical mating behaviors and secondary sex characters (SSCs) were affected [59]. This result indicates the role of *Eczbtb40* inspermatogenesis on secondary side. However, the specific function of *zbtb40* requires further analysis in the whole process of spermatogenesis.

Conclusions

In the present study, four cell types (SG, SC, ST, and SZ) were captured in the process of spermatogenesis in orange-spotted grouper induced by artificial MT implantation. An optimized protocol was developed to separate different male germ cells in orange-spotted grouper by LCM. Through the transcriptome analysis, the expressional patterns of related genes in spermatogenesis were explored and *Eczbtb40* was investigated.

Methods

Animals

Orange-spotted groupers were obtained from Guangdong Daya Bay Fishery Development Center (Huizhou 516081, Guangdong, China). The fish were kept in indoor pools under controlled water temperatures of 22.7~27.8 °C. All fish were anesthetized with MS222 until death in 10-20 minutes, then the fish were sacrificed. All animal experiments conducted were in accordance with the guidelines and approval of the respective Animal Research and Ethics Committees of Sun Yat-Sen University.

MT-induced sex reversal

In this study, the sex reversal was artificially inducted by MT (Sigma, USA) treatment. The fabrication of the slow-release strips and steps of MT implantation were referred to our previous paper with minor modification [60]. Fish (body weight, 1.90 ± 0.65 kg; body length, 43.75 ± 9.25 cm) were divided into two groups, sham group (n = 15) and MT implantation group (n = 15). The dosage of MT was 10 mg/kg body weight. Before implantation (Week 0), gonadal tissues of five fish were collected randomly. After MT implantation, five fish were sampled randomly every week respectively from two groups until 3 weeks. For each fish, one piece of gonadal tissue was fixed in Bouin's solution for histological examination of the development stage of the gonad, another piece of the gonad was immobilized by 4% paraformaldehyde for florescence in situ hybridization (FISH), the other piece of gonadal tissue was embedded with OCT (Sakura, USA) then frozen immediately in liquid nitrogen for LCM. All the other tissues were frozen immediately in liquid nitrogen, and then stored at -80 °C until further use.

Histology analysis

Gonadal tissues were embedded in paraffin after being fixed 24 h in Bouin's solution. The embedded blocks were sectioned at 5~6 μm and stained with hematoxylin and eosin (H&E). The gonadal sections were classified by light microscopy.

Visualization of the target cells

There are several factors influencing the RNA quality in the process of visualization, including the samplecryostat sections (the quality of fresh and quick-frozen samples usually is more optimal than fixed tissues), the complex histopathology, and issues arising from the staining, and so on.

Cryostat sections of gonad for LCM

The RNase-free Membrane Slides (MMI, Switzerland) as a slide to mount the cryosections. A series of procedures were produced before sectioning. The slides were incubated in super clean bench under ultraviolet (UV) radiation for 30 min. Then the slides disposed of with 0.1mg/ml polylysine (Sigma, USA) for 5 min, after that rinsed slide by 0.1 % DEPC ((Sigma, USA, Diethyl pyrophosphate). At last, the slides dried and stored at a sealed box for further use [5].

Before sectioning, the microtome (Leica, Germany) was wiped down with RNase inhibitor (Ambion®, USA) to avoid cross-contamination, and a new blade (Lecia, Germany) treated with RNase inhibitor was used to cut each sample. The gonad blocks were put into Leica Microtomes 30 minutes to adjust the sectioning temperature (-20 °C~ -25 °C). The ovary was cryosectioned at 7 μm, and the testis was cryosectioned at 6 μm.

Cryosections Staining

After being desiccated for one minute, the sections stained by H&E Staining Kit Plus (MMI, Switzerland). The procedures were referred to instructions of the Kit and taken some adjustments to make sure the optimization of RNA quality. However, the sections of the two groups were performed different staining protocols. The whole process was controlled in 30 minutes [61].

Laser Capture Microdissection

First of all, all facilities and tools were wiped by RNase inhibitor. General sterile glass slides were put under the Membrane Slides as supported slides. Once the stained slides exposed in air, the surface of the slide emerged massive water droplets which accelerate degradation of RNA. Thus the whole process of microdissection must control in one hour, and dry the sections quickly. Then load the slides and LCM caps (diffuser caps, MMI, Switzerland) to laser micro-cutting instrument (MMI, CellCut Plus, Switzerland). Find the cells of interest through adjusting microscope, at the same time optimize three important parameters (cell velocity, laser focus, and laser power). After circling the interesting area, the laser starts to capture the cells as many as possible. At last, unload of caps containing the captured tissue, and add 50 μl TPK Lysis Buffer (Micro Elute® RNA Kit, Omega, USA) immediately. Extract RNA instantly or store diffuser caps in −80 °C (<2 days).

RNA extraction

The procedures of RNA extraction were referred to as instructions of Micro Elute® RNA Kit (Omega, USA) with some adjustment.

Library preparation for transcriptome sequencing

A total amount of 1.5 μg RNA per sample was used as input material for the RNA sample preparation. NEBNext® Ultra™ RNA Library Prep Kit were used to generate sequencing libraries for Illumina® (NEB, USA) following the manufacturer's recommendations. And index codes were added to attribute sequences to each sample. Briefly, mRNA was purified from total RNA using poly-T oligo-attached magnetic beads. Fragmentation was carried out by divalent cations under elevated temperature in NEB Next First-Strand Synthesis Reaction Buffer (5X). First strand cDNA was synthesized using random hexamer primer and M-MuLV Reverse Transcriptase (RNase H^-). Second strand cDNA synthesis used DNA Polymerase I and RNase H subsequently. Remaining overhangs were converted into blunt ends via exonuclease/polymerase activities. After adenylation of 3’ ends of DNA fragments, NEB Next Adaptor with hairpin loop structure was ligated to prepare for hybridization. In order to select cDNA fragments of preferentially 150~200 bp in length, the library fragments were purified with AMPure XP system (Beckman Coulter, Beverly, USA). Then 3 μl USER Enzyme (NEB, USA) was used with size-selected, adaptor-ligated cDNA at 37°C for 15 min followed by 5 min at 95 °C before PCR. Then PCR was performed with Phusion High-Fidelity DNA polymerase, Universal PCR primers, and Index (X) Primer. At last, PCR products were purified (AMPure XP system) and library quality was assessed on the Agilent Bioanalyzer 2100 system.

The clustering of the index-coded samples was performed on a cBot Cluster Generation System using TruSeq PE Cluster Kit v3-cBot-HS (Illumina) according to the manufacturer’s instructions. After cluster generation, the library preparations were sequenced on an Illumina Hiseq platform and 150 bp paired-end reads were generated.

Processing of raw reads and quantification of differential gene expression levels

Raw data (raw reads) of the fastq format were first processed through in-house Perl scripts. In this step, clean data (clean reads) were obtained by removing reads containing adapter, reads containing ploy-N and low quality reads from raw data. At the same time, Q20, Q30 and GC content the clean data were calculated. Q20 indicates that every 100 bp of sequencing reads will have an error, and Q30 indicates that every 1000 bp of sequencing reads will have an error. All the downstream analyses were based on clean data with high quality.

The clean reads were mapped to the orange-spotted grouper (*E. coioides*) genome (Zhang Y. et al., unpublished data; using SOAP aligner 2.0 [62]), which has been de novo assembled. Index of the reference genome was built using Bowtie v2.2.3 and paired-end clean reads were aligned to the reference genome using TopHat v2.0.12. We selected TopHat as the mapping tool for that TopHat can generate a

database of splice junctions based on the gene model annotation file and thus a better mapping result than other non-splice mapping tools.

HTSeq v0.6.1 was used to count the reads numbers mapped to each gene. And then FPKM of each gene was calculated based on the length of the gene and reads count mapped to this gene. FPKM, expected number of Fragments Per Kilobase of transcript sequence per Millions of base pairs sequenced, considers the effect of sequencing depth and gene length for the reads count at the same time, and is currently the most commonly used method for estimating gene expression levels [63].

Differential expression genes analysis

Prior to differential gene expression analysis, for each sequenced library, the read counts were adjusted by edgeR program package through one scaling normalized factor. Differential expression analysis of two conditions was performed using the DEGSeq R package (1.20.0). The P values were adjusted using the Benjamini & Hochberg method. Corrected P-value of 0.005 and log 2 (Fold change) of 1 were set as the threshold for significant differential expression.

GO and KEGG enrichment analysis of differentially expressed genes

Gene Ontology (GO) enrichment analysis of differentially expressed genes was implemented by the GOseq R package, in which gene length bias was corrected. GO terms with corrected P value less than 0.05 were considered significantly enriched by differential expressed genes. The identified DEGs were conducted for enrichment analysis subsequently by GO: Termfinder software using the hypergeometric test [64, 65], and P-values were corrected using the Bonferroni method [57]. Being selected significantly enriched GO terms with Q-value < 0.05.

KEGG is a database resource for understanding high-level functions and utilities of the biological system, such as the cell, the organism and the ecosystem, from molecular-level information, especially large-scale molecular datasets generated by genome sequencing and other high-through put experimental technologies (http://www.genome.jp/kegg/). We used KOBAS software to test the statistical enrichment of differential expression genes in KEGG pathways.

Different expression genes analyzed by real-time PCR

To validate the accordance with those genes inferred from RNA-seq data, the relative mRNA levels of 13 differentially expressed genes (*nr0b1*, *era*, *erb*, *wnt9*, *gdf9*, *bmp15*, *cyp17a1*, *3hd*, *sdr12*, *sdr11*, *p5cdh*, *cyp3a40*, and *sdr13*) were examined by quantitative real-time PCR (RT-PCR) in sex reversal of orange-spotted grouper. Total RNA of gonad was extracted by TRIzol (Invitrogen, USA) and then 1 μg RNA from each sample was reverse transcribed with random primers by using the First Strand cDNA Synthesis Kit (Roche, USA) according to the manufacturer's instruction. The RT-PCR reaction was performed in a 10 μl reaction volume using the SYBR Green PCR master mix (Roche, USA). The amplification regime was 95 °C for 5 min, followed by 40 cycles of amplification at 95 °C for 10 s, 58 °C for 15 s and 72 °C for 20 s. The specificity of RT-PCR amplification was confirmed by melt-curve analysis, agarose gel

electrophoresis, and sequencing of PCR products. All mRNA quantification data were normalized to *ef1a* and presented as a relative control group. The specific primers used in this study were listed in Table 3.

Open Reading Frame (ORF) cloning and sequence analysis of *Eczbtb40* cDNAs

Total RNA of the gonad was extracted by TRIzol (Invitrogen, USA). RNA was reversed to cDNAs with First Strand cDNA Synthesis Kit (Roche, USA). The reverse transcription process was as follow 37 °C for 15 min, 98 °C for 5 min, 4 °C for 5 min. The amplification regime was 35 cycles of 94 °C for 20 s, 55 °C for 10 s, and 72 °C for 20 s, followed by further amplification at 72 °C for 5 min. Based on the cDNA fragments in RNA-seq data, specific upstream and downstream primers (Table 2) were designed. The primers were used to amplify the ORFs of *Eczbtb40*. The PCR amplification procedures were performed as follows: denaturation at 94 °C for 2 min, followed by 35 cycles at 94 °C for 30 s, 52~58 °C (depending on the melting temperature of primers) for 30 s, and 68 °C for 1min. The reactions were completed with a final extension of 10 min at 68 °C. To separate the desired band in the amplification product, 2% agarose gel electrophoresis was used, and the band of the desired size was purified by the E.Z.N.A. Gel Extraction Kit (Omega, USA). The purified product was then subcloned into the pGEM-Easy vector (Fermentas, USA). According to the sequencing result, the ORFs of *Eczbtb40* were obtained.

The putative amino acid sequences were predicted by DNAMAN software and multiple sequence alignments of amino acids were performed in the ClustalX (1.81) software. Meanwhile, protein phylogenetic analysis was conducted with MEGAX using the method of neighbor-joining method and the top ten motif sites were predicted by motif-based sequence analysis tools (MEME).

Tissue distribution of *Eczbtb40*

To detect the tissue distribution of *Eczbtb40*, eight tissues were dissected, including whole brain, heart, head kidney, liver, kidney, pituitary, ovary, and testis. Total RNA from eight tissues was extracted. RNA was reversed to cDNA with First Strand cDNA Synthesis Kit (Roche, USA). The reverse transcription process was as follow 37 °C for 15 min, 98 °C for 5 min, 4 °C for 5 min. The amplification regime was 35 cycles of 94 °C for 20 s, 55 °C for 10 s, and 72 °C for 20 s, followed by further amplification at 72 °C for 5 min. The specific primers used in this study were listed in Table 2.

Expression profile of *Eczbtb40* in gonads during MT-induced sex reversal

The expression profiles of *Eczbtb40* in the gonad were detected by RT-PCR during MT-induced sex reversal.

In situ localization of *Eczbtb40* in gonads during MT-induced sex reversal

Fluorescence in situ localization (FISH) referred to previous papers with minor modifications [66]. The DIG label was tested with an alkaline phosphatase conjugated Flu-anti-DIG antibody (Roche Diagnostics; diluted 1:1000) and colored the signal with Fluorescence Systems (Roche, USA), and sections were counterstained by 4'6-diamidino-2-phenylindole (DAPI) for cell nuclear staining to confirm the number

and status of germ cell. At last, sections were mounted with the Gold Anti-fade reagent (Invitrogen, USA) and imaged by laser scanning confocal microscope (Leica TCS-SP5, Germany).

Dual-label in situ hybridization of *Eczbtb40* and *Eccyp17a1* in gonads

The protocol of dual-label in situ hybridization of *Eczbtb40* and *Eccyp17a1* was referred to previous study [67]. Expression of *Eczbtb40* was performed using digoxigenin (DIG)-labeled mRNA probes in combination with biotin-labeled *Eccyp17a1* mRNA probes.

Statistical analysis

All data were expressed as mean values ± SEM. Significant differences were checked by one-way analysis of variance (ANOVA) and student's t-test was used, and a probability level less than 0.05 ($P < 0.05$) was used to indicate significance. All data were performed using GraphPad Prism5.0 (GraphPad Software, San Diego, CA) and analyzed by SPSS17.0 (SPSS, Chicago, IL, USA).

Abbreviations

KEGG: Kyoto encyclopedia of genes and genomes database

RNA: Ribonucleic Acid

cDNA: complementary deoxyribonucleic acid

PCR: Polymerase Chain Reaction kg: kilogram cm: centimeter

PBS: phosphate buffered solution DEPC: diethyl pyrocarbonate

μm: micrometer μg: microgram ml: milliliter μl: microliter

min: minute s: second h: hour

Tris-HCl: Tris (hydroxymethyl) aminomethane

NaCl: Sodium chloride PH: potential of hydrogen

NBT: Nitro-Blue-Tetrazolium BCIP: 5-bromo-4-chloro-3-indolyl-phosphate

Declarations

Ethics approval and consent to participate

All the procedures in this manuscript had been approved by the Committee for Animal Experiments in Sun Yat-Sen University, China. The methods used in this study were carried out in accordance with the Laboratory Animal Management Principles of China.

p>Consent for publication

Not applicable.

Competing interests

The authors declare that they have no competing interests.

Funding

This work was supported by Natural Science Foundation of China (u1401213, 31802266), Special Fund for Agro-scientific Research in the Public Interest (201403011), Yang Fan Innovative & Entrepreneurial Research Team Project (No.201312H10), the Program of the China-ASEAN Maritime Cooperation Fund of the Chinese government, and China Agriculture Research System (ARS-47). The funding body didn't play any roles in the design of the study and collection, analysis, and interpretation of data and in writing the manuscript.

Availability of data and materials

The datasets used and analyzed during the current study available from the corresponding author on reasonable request.

Authors' contributions

XW and YY analyzed the sequencing data; XW, CYZ and YG collected and prepared the samples; XW wrote the manuscript; SSL and XCL supervised the study. All authors read and approved the final manuscript for publication.

Acknowledgment

Many thanks to Mr. Yu Chen, and this project was supported by Miss. Meifeng Liu and Ling Qu for their assistance in fish rearing and sample collection.

Publisher's Note

Springer Nature remains neutral with regard to jurisdictional claims in published maps and institutional affiliations.

References

1. Wang Z, Gerstein M, Snyder M: RNA-Seq: a revolutionary tool for transcriptomics. *Nature Reviews Genetics* 2009, 10(1):57-63.

2. Datta S, Malhotra L, Dickerson R, Chaffee S, Sen CK, Roy S: Laser capture microdissection: Big data from small samples. *Histology and Histopathology* 2015, 30(11):1255-1269.

3. Wiener MC, Sachs JR, Deyanova EG, Yates NA: Differential mass spectrometry: a label-free LC-MS method for finding significant differences in complex peptide and protein mixtures. *Analytical Chemistry* 2004, 76(20):6085-6096.

4. Falko Fend MR: Laser capture microdissection in pathology. *Journal of Clinical Pathology* 2015, 2000(53):666–672.

5. Blokhina O, Valerio C, Sokołowska K, Zhao L, Kärkönen A, Niittylä T, Fagerstedt K: Laser Capture Microdissection Protocol for Xylem Tissues of Woody Plants. *Frontiers in Plant Science* 2017, 7(1965):1-14.

6. Bonnet A, Bevilacqua C, Benne F, Bodin L, Cotinot C, Liaubet L, Sancristobal M, Sarry J, Terenina E, Martin P *et al*: Transcriptome profiling of sheep granulosa cells and oocytes during early follicular development obtained by laser capture microdissection. *BMC Genomics* 2011, 12:417.

7. Holland-Staley FKXZCA: The -omics Era and Its Impact. *Advances in the Science of Pathology* 2004, 128:1337-1345.

8. Farris S, Wang Y, Ward JM, Dudek SM: Optimized Method for Robust Transcriptome Profiling of Minute Tissues Using Laser Capture Microdissection and Low-Input RNA-Seq. *Frontiers in Molecular Neuroscience* 2017, 10:1-13.

9. Bonner RF E-BM, Cole K, Pohida T, Chuaqui R, Goldstein S, Liotta LA: Cell sampling: laser capture microdissection: molecular analysis of tissue. *Science* 1997, 278:1481-1483.

10. Sluka P, O'Donnell L, Stanton PG: Stage-specific expression of genes associated with rat spermatogenesis: characterization by laser-capture microdissection and real-time polymerase chain reaction. *Biology of Reproduction* 2002, 67(3):820-828.

11. Sluka P, O'Donnell L, McLachlan RI, Stanton PG: Application of laser-capture microdissection to analysis of gene expression in the testis. *Progress in Histochemistry and Cytochemistry* 2008, 42(4):173-201.

12. Vinas J, Piferrer F: Stage-specific gene expression during fish spermatogenesis as determined by laser-capture microdissection and quantitative-PCR in sea bass (*Dicentrarchus labrax*) gonads. *Biology of Reproduction* 2008, 79(4):738-747.

13. Jørgensen A, Nielsen JE, Nielsen BF, Morthorst JE, Bjerregaard P, Leffers H: Expression of prostaglandin synthases (pgds and pges) during zebrafish gonadal differentiation. *Comparative Biochemistry and Physiology Part A: Molecular & Integrative Physiology* 2010, 157(1):102-108.

14. Xiaochun Liu PZ, Kathy W.Y. Sham, Jacky M.L. Yuen, Chuanming Xie, Yong Zhang, Yun Liu, Shuisheng Li, Xigui Huang, Christopher H.K. Cheng, and Haoran Lin: Identification of a Membrane

Estrogen Receptor in Zebrafish with Homology to Mammalian GPER and Its High Expression in Early Germ Cells of the Testis. *Biology of Reproduction* 2009, 80:1253–1261.

15. Jorgensen A, Nielsen JE, Morthorst JE, Bjerregaard P, Leffers H: Laser capture microdissection of gonads from juvenile zebrafish. *Reproductive Biology Endocrinology* 2009, 7(97):1-7.

16. Garcia-Lopez A, Bogerd J, Granneman JC, van Dijk W, Trant JM, Taranger GL, Schulz RW: Leydig cells express follicle-stimulating hormone receptors in African catfish. *Endocrinology* 2009, 150(1):357-365.

17. Liu M, de Mitcheson YS: Gonad development during sexual differentiation in hatchery-produced orange-spotted grouper (*Epinephelus coioides*) and humpback grouper (Cromileptes altivelis) (Pisces: Serranidae, Epinephelinae). *Aquaculture* 2009, 287(1-2):191-202.

18. Schulz RW, de Franca LR, Lareyre JJ, Le Gac F, Chiarini-Garcia H, Nobrega RH, Miura T: Spermatogenesis in fish. *General and Comparative Endocrinology* 2010, 165(3):390-411.

19. Miura2 RWST: Spermatogenesis and its endocrine regulation. *Fish Physiology and Biochemistry* 2002, 26:43–56.

20. Nakamura N, Shibata H, O'Brien DA, Mori C, Eddy EM: Spermatogenic cell-specific type 1 hexokinase is the predominant hexokinase in sperm. *Mocular Reproduction and Development* 2008, 75(4):632-640.

21. Eric L. Bittman LD, Liyue Huang, and Allison Paroskie: Period gene expression in mouse endocrine tissues. *American Jouranl of Physiology Regulatory Integrative Comparative Physiology* 2003, 285: R561–R569.

22. Harvey S, Baudet ML, Murphy A, Luna M, Hull KL, Aramburo C: Testicular growth hormone (GH): GH expression in spermatogonia and primary spermatocytes. *General and Comparative Endocrinology* 2004, 139(2):158-167.

23. Chan WY, Lee TL, Wu SM, Ruszczyk L, Alba D, Baxendale V, Rennert OM: Transcriptome analyses of male germ cells with serial analysis of gene expression (SAGE). *Molecular and Cellular Endocrinology* 2006, 250(1-2):8-19.

24. Yao J, Chiba T, Sakai J, Hirose K, Yamamoto M, Hada A, Kuramoto K, Higuchi K, Mori M: Mouse testis transcriptome revealed using serial analysis of gene expression. *Mammalian Genome* 2004, 15(6):433-451.

25. LOIR M: Spermatogonia of rainbow trout II. In vitro study of the influence of pituitary hormones, growth factors and steroids on mitotic activity. *Molecular Reproduction and Development* 1999, 53:434–442.

26. Beis D, Stainier DY: In vivo cell biology: following the zebrafish trend. *Trends in Cell Biology* 2006, 16(2):105-112.

27. Stogios PJ, Downs GS, Jauhal JJ, Nandra SK, Prive GG: Sequence and structural analysis of BTB domain proteins. *Genome Biology* 2005, 6(R82).

28. van Roy FM, McCrea PD: A role for Kaiso-p120ctn complexes in cancer? *Nature* 2005, 5(12):956-964.

29. Lovelace DL, Gao Z, Mutoji K, Song YC, Ruan J, Hermann BP: The regulatory repertoire of PLZF and SALL4 in undifferentiated spermatogonia. *Development* 2016, 143(11):1893-1906.

30. Costoya JA, Hobbs RM, Barna M, Cattoretti G, Manova K, Sukhwani M, Orwig KE, Wolgemuth DJ, Pandolfi PP: Essential role of Plzf in maintenance of spermatogonial stem cells. *Nature Genetics* 2004, 36(6):653-659.

31. Ozaki Y, Saito K, Shinya M, Kawasaki T, Sakai N: Evaluation of Sycp3, Plzf and Cyclin B3 expression and suitability as spermatogonia and spermatocyte markers in zebrafish. *Gene Expression Patterns* 2011, 11(5-6):309-315.

32. Buaas FW, Kirsh AL, Sharma M, McLean DJ, Morris JL, Griswold MD, de Rooij DG, Braun RE: Plzf is required in adult male germ cells for stem cell self-renewal. *Nature Genetics* 2004, 36(6):647-652.

33. Lacerda SM, Costa GM, de Franca LR: Biology and identity of fish spermatogonial stem cell. *General and Comparative Endocrinology* 2014, 207:56-65.

34. Boonanuntanasarn S, Bunlipatanon P, Ichida K, Yoohat K, Mengyu O, Detsathit S, Yazawa R, Yoshizaki G: Characterization of a vasa homolog in the brown-marbled grouper (*Epinephelus fuscoguttatus*) and its expression in gonad and germ cells during larval development. *Fish Physiology and Biochemistry* 2016, 42(6):1621-1636.

35. Wu X, Qu L, Li S, Guo Y, He J, Liu M, Liu X, Lin H: Molecular characterization and expression patterns of stem-loop binding protein (SLBP) genes in protogynous hermaphroditic grouper, Epinephelus coioides. *Gene* 2019, 700:120-130.

36. Wang Q, Liu Y, Peng C, Wang X, Xiao L, Wang D, Chen J, Zhang H, Zhao H, Li S *et al*: Molecular regulation of sex change induced by methyltestosterone -feeding and methyltestosterone -feeding withdrawal in the protogynous orange-spotted grouper. *Biology of Reproduction* 2017, 97(2):324-333.

37. Jensen EC: Laser capture microdissection. *The Antomical Record* 1996(296):1683–1687.

38. Holger Knaut FP, Kerstin Bohmann, Heinz Schwarz, and Christiane Nüsslein-Volhard: Zebrafish vasa RNA but Not Its Protein Is a Component of the Germ Plasm and Segregates Asymmetrically before Germline Specification. *The Journal of Cell Biology* 2000, 149(4):875–888.

39. Wen-Xia He MW, Zhen Liu, Zhi Li, Yang Wang, Jian Zhou, Peng Yu, Xiao-Juan Zhang, Li Zhou and Jian-Fang Gui: Oocyte-specific maternal Slbp2 is required for replication-dependent histone storage and early nuclear cleavage in zebrafish oogenesis and embryogenesis. *RNA* 2018, 24(12):1738-1748.

40. Xia W, Zhou L, Yao B, Li CJ, Gui JF: Differential and spermatogenic cell-specific expression of DMRT1 during sex reversal in protogynous hermaphroditic groupers. *Molecular and Cellular Endocrinology* 2007, 263(1-2):156-172.

41. Marin-Juez R, Vinas J, Mechaly AS, Planas JV, Piferrer F: Stage-specific gene expression during spermatogenesis in the Senegalese sole (*Solea senegalensis*), a fish with semi-cystic type of spermatogenesis, as assessed by laser capture microdissection and absolute quantitative PCR. *Gen Comp Endocrinol* 2013, 188:242-250.

42. Haugen T, Almeida FF, Andersson E, Bogerd J, Male R, Skaar KS, Schulz RW, Sorhus E, Wijgerde T, Taranger GL: Sex differentiation in Atlantic cod (*Gadus morhua L.*): morphological and gene expression studies. *Reproductive Biology and Endocrinology* 2012, 10:47.

43. von Schalburg KR, Yasuike M, Yazawa R, de Boer JG, Reid L, So S, Robb A, Rondeau EB, Phillips RB, Davidson WS *et al*: Regulation and expression of sexual differentiation factors in embryonic and extragonadal tissues of Atlantic salmon. *BMC Genomics* 2011, 12(31).

44. Chen S, Zhang H, Wang F, Zhang W, Peng G: nr0b1 (DAX1) mutation in zebrafish causes female-to-male sex reversal through abnormal gonadal proliferation and differentiation. *Molecular and Cellular Endocrinology* 2016, 433:105-116.

45. Wang D TK, Balasubramanian Senthilkumaran, Fumie Sakai, Cheni Chery Sudhakumari, Taiga Suzuki, Michiyasu Yoshikuni, Masaru Matsud, Ken-ichirou Morohashi, and Yoshitaka Nagahama: Molecular cloning of DAX1 and SHP cDNAs and their expression patterns in the Nile tilapia, *Oreochromis niloticus*. *Biochemical and Biophysical Research Communications* 2002, 297:632–640.

46. Martins RS, Deloffre LA, Mylonas CC, Power DM, Canario AV: Developmental expression of DAX1 in the European sea bass, Dicentrarchus labrax: lack of evidence for sexual dimorphism during sex differentiation. *Reproductive Biology Endocrinology* 2007, 5(19):1-13.

47. Hu Q, Guo W, Gao Y, Tang R, Li D: Molecular cloning and characterization of amh and dax1 genes and their expression during sex inversion in rice-field eel *Monopterus albus*. *Scientific Reports* 2015, 5(16667).

48. Li H, Zhang Z, Bi Y, Yang D, Zhang L, Liu J: Expression characteristics of beta-catenin in scallop Chlamys farreri gonads and its role as a potential upstream gene of Dax1 through canonical Wnt signalling pathway regulating the spermatogenesis. *PLoS One* 2014, 9(12).

49. KORACH JFCAKS: Estrogen Receptor Null Mice: What Have We Learned and Where Will They Lead Us? *Endocrine Reviews* 1999, 20(3):358–417.

50. George G. J. M. Kuiper EE, Markku Pelto-Huikko, Stefan Nilsson, and Jan-Ake Gustafsson: Cloning of a novel estrogen receptor expressed in rat prostate and ovary. *Proceedings of the National Academy of Sciences of the United States of America* 1996, 93:5925-5930.

51. Comparison of the Ligand Binding Specificity and Transcript Tissue Distribution of Estrogen Receptors-annotated. *Endocrinology*, 138:863-870.

52. Hui Zhang† JST, Lotta Johansson, Jan-Åke Gustafsson and Eckardt Treuter: DAX-1 Functions as LXXLL-Containing Corepressor for Activated Estrogen Receptors. *The Journal of Biological Chemistry*, 275(51):39855–39859.

53. Miller JR: The Wnts. *Genome Biology* 2001, 3(1):3001.3001–3001.3015.

54. Sanfins A, Rodrigues P, Albertini DF: GDF-9 and BMP-15 direct the follicle symphony. *Journal of Assisted Reproduction and Genetics* 2018, 35(10):1741-1750.

55. Susan L. Fitzpatrick DMS, Paul J. Shughrue, Malcolm V. Lane, Istvan J. Merchenthaler, and Donald E. Frail: Expression of growth differentiation factor-9 messenger ribonucleic acid in ovarian and nonovarian rodent and human tissues. *Endocrinology* 1998, 139(5):2571-2577.

56. Nicholls PK, Harrison CA, Gilchrist RB, Farnworth PG, Stanton PG: Growth differentiation factor 9 is a germ cell regulator of Sertoli cell function. *Endocrinology* 2009, 150(5):2481-2490.

57. Johanna Aaltonen MPL, Kaisa Vuojolainen, Risto JAATINEN, Nina Horelli-Kuitunen, Laura Seppa , Henna Louhio, Timo Tuuri, Jari Sjoberg, Ralf Butzow, Outi Hovatta, Leslie Dale, and Olli Rivtos: Human Growth Differentiation Factor 9 (GDF-9) and Its Novel Homolog GDF-9B Are Expressed in Oocytes during Early Folliculogenesis. *The Journal of Clinical Endocrinology & Metabolism* 1999, 84(8):2744-2750.

58. Clelland E, Kohli G, Campbell RK, Sharma S, Shimasaki S, Peng C: Bone morphogenetic protein-15 in the zebrafish ovary: complementary deoxyribonucleic acid cloning, genomic organization, tissue distribution, and role in oocyte maturation. *Endocrinology* 2006, 147(1):201-209.

59. Zhai G, Shu T, Xia Y, Lu Y, Shang G, Jin X, He J, Nie P, Yin Z: Characterization of Sexual Trait Development in cyp17a1-Deficient Zebrafish. *Endocrinology* 2018, 159(10):3549-3562.

60. Shi Y, Zhang Y, Li S, Liu Q, Lu D, Liu M, Meng Z, Cheng CH, Liu X, Lin H: Molecular identification of the Kiss2/Kiss1ra system and its potential function during 17alpha-methyltestosterone-induced sex reversal in the orange-spotted grouper, Epinephelus coioides. *Biology of Reproduction* 2010, 83:63-74.

61. Golubeva Y, Salcedo R, Mueller C, Liotta LA, Espina V: Laser capture microdissection for protein and NanoString RNA analysis. *Methods in Molecular Biology* 2013, 931:213-257.

62. R. Luo BL, Y. Xie, Z. Li, W. Huang, J. Yuan, G. He, Y. Chen, Q. Pan, Y. Liu, J. Tang, G. Wu, H. Zhang, Y. Shi, Y. Liu, C. Yu, B. Wang, Y. Lu, C. Han, DW. Cheung, S. Yiu, S. Peng, X. Zhu, G. Liu, X. Liao, Y. Li, H. Yang, J. Wang, T. Lam and J. Wang: SOAPdenovo2: an empirically improved memory-efficient short-read de novo assembler. *GigaScience* 2012, 1.

63. Trapnell C, Williams BA, Pertea G, Mortazavi A, Kwan G, van Baren MJ, Salzberg SL, Wold BJ, Pachter L: Transcript assembly and quantification by RNA-Seq reveals unannotated transcripts and isoform switching during cell differentiation. *Nature Biotechnology* 2010, 28(5):511-515.

64. Flight RM, Wentzell PD: Potential bias in GO::TermFinder. *Briefs in Bioinformatics* 2009, 10(3):289-294.

65. Boyle EI, Weng S, Gollub J, Jin H, Botstein D, Cherry JM, Sherlock G: GO::TermFinder–open source software for accessing Gene Ontology information and finding significantly enriched Gene Ontology terms associated with a list of genes. *Bioinformatics* 2004, 20(18):3710-3715.

66. Xu H, Gui J, Hong Y: Differential expression of vasa RNA and protein during spermatogenesis and oogenesis in the gibel carp (*Carassius auratus gibelio*), a bisexually and gynogenetically reproducing vertebrate. *Developmental Dynamics* 2005, 233(3):872-882.

67. Guo Y, Wang Q, Li G, He M, Tang H, Zhang H, Yang X, Liu X, Lin H: Molecular mechanism of feedback regulation of 17beta-estradiol on two kiss genes in the protogynous orange-spotted grouper (*Epinephelus coioides*). *Molecular Reprodution Development* 2017, 84(6):495-507.

Figure Legends

Fig. 1. Histological effects of MT treatment on gonads of the orange-spotted grouper. (A, B, D and F) Histology of gonads in control fish. (C, E and G) Histology of gonads after MT implantation. PO, primary-growth stage oocyte; PVO, the cortical-alveolus stage oocyte; SG, spermatogonia; SC, spermatocyte; ST, spermatid; and SZ, spermatozoa. Scale bars = 50 um.

Fig. 2. Gonadal structure by different staining methods. (A) Histological structure of gonad in MT treatment by H&E staining. (B) Histological structure of fresh gonad in MT treatment by cry-sectioning. SG, spermatogonia; SC, spermatocyte; ST, spermatid; SZ, spermatozoa; and PO, primary-growth stage oocyte. Scale bars = 20 um.

Fig. 3. Expression of several sex-related genes and tissue distribution of *Eczbtb40*. (A) Expression of several sex-related genes in four cell types by laser capture. *Ef1a* was used as the reference gene. M, maker 2000; C+, the cDNA of ovaries (stayed at the stage with the portion of mostly PO) as a positive control; C-, template-free as a negative control; SG, spermatogonia; SC, spermatocyte; ST, spermatid; SZ, spermatozoa. (B) Tissue distribution of *Eczbtb40* in orange-spotted grouper. The ovaries of the fish stayed at the stage with the portion of mostly primary-growth stage oocytes (PO) and the testis from the mature male. *Ef1a* was used as the reference gene. M, maker 2000; 1, the whole brain; 2, heart; 3, head kidney; 4, liver; 5, kidney; 6, pituitary; 7, ovary; 8, testis.

Fig. 4. Analysis data of transcriptome. (A) The top 20 pathways in KEGG analysis with the significant difference. (B) A heat map was constructed based on the selected genes. Red indicated high expression and green low expression.

Fig. 5. Validation of selected genes using RT-PCR. (A) nuclear receptor subfamily 0 group B member 1 (*nr0b1*); (B) estrogen receptor alpha (*era*); (C) estrogen receptor beta (*erb*); (D) protein Wnt-9 (*wnt9*); (E) growth and differentiation factor 9 (*gdf9*); (F) Bone morphogenetic protein 15 (*bmp15*).

Fig. 6. Validation of selected genes using RT-PCR. (A) Steroid 17-alpha-hydroxylase (*cyp17a1*); (B) 3-hydroxyisobutyrate dehydrogenase (*3hd*); (C) dehydrogenase/reductase (SDR) family member 12 (*sdr12*); (D) SDR family member 11 (*sdr11*); (E) delta-1-pyrroline-5-carboxylate dehydrogenase (*p5cdh*); (F) cytochrome P450 3A30-like (*cyp3a30*); (G) SDR family member 13 (*sdr13*); (H) zinc finger and BTB domain containing 16 (*zbtb40*).

Fig. 7. Phylogenetic relationships and conserved DNA motifs in *zbtb40* genes from 14 species. (A) Phylogenetic tree of *zbtb40*swere conducted by MEGAX using the neighbor-joining likelihood method with 500 bootstrap replicates. Numerals at nodes were bootstrap values. The species names are followed by sequence accession numbers. (B) The top ten motif composition of *zbtb40*s. The motifs, numbers 1–10, are displayed in different colored boxes. The sequence information for each motif is provided in Supplementary table 1.

Fig. 8. ISH analysis the *Eczbtb40* mRNA expression in gonads at the sex reversal process by artificial MT implantation. (A) Gonadal stage with the portion of mostly primary-growth stage oocytes, (B) gonadal stage after one weeks of MT implantation, (C) gonadal stage after two weeks of MT implantation, (D) gonadal stage after three weeks of MT implantation. Red signals indicate *Eczbtb40*, blue staining indicates nuclei. PO, primary-growth stage oocyte; ST, spermatids; SZ, spermatozoa. Scale bars = 50 μm.

Fig. 9. Co-localization of *Eczbtb40* and *Eccyp17a1* by FISH in the gonad of ovary (A-D) and testis (E-H). Gonad sections were stained red for *Eczbtb40* mRNA, green for *Eccyp17a1* mRNA and blue for DAPI. Red and green colors generated a yellow color. PO, primary-growth stage oocyte; SG, spermatogonia; SC, spermatocyte; ST, spermatid. Scale bars = 25 μm.

Figures

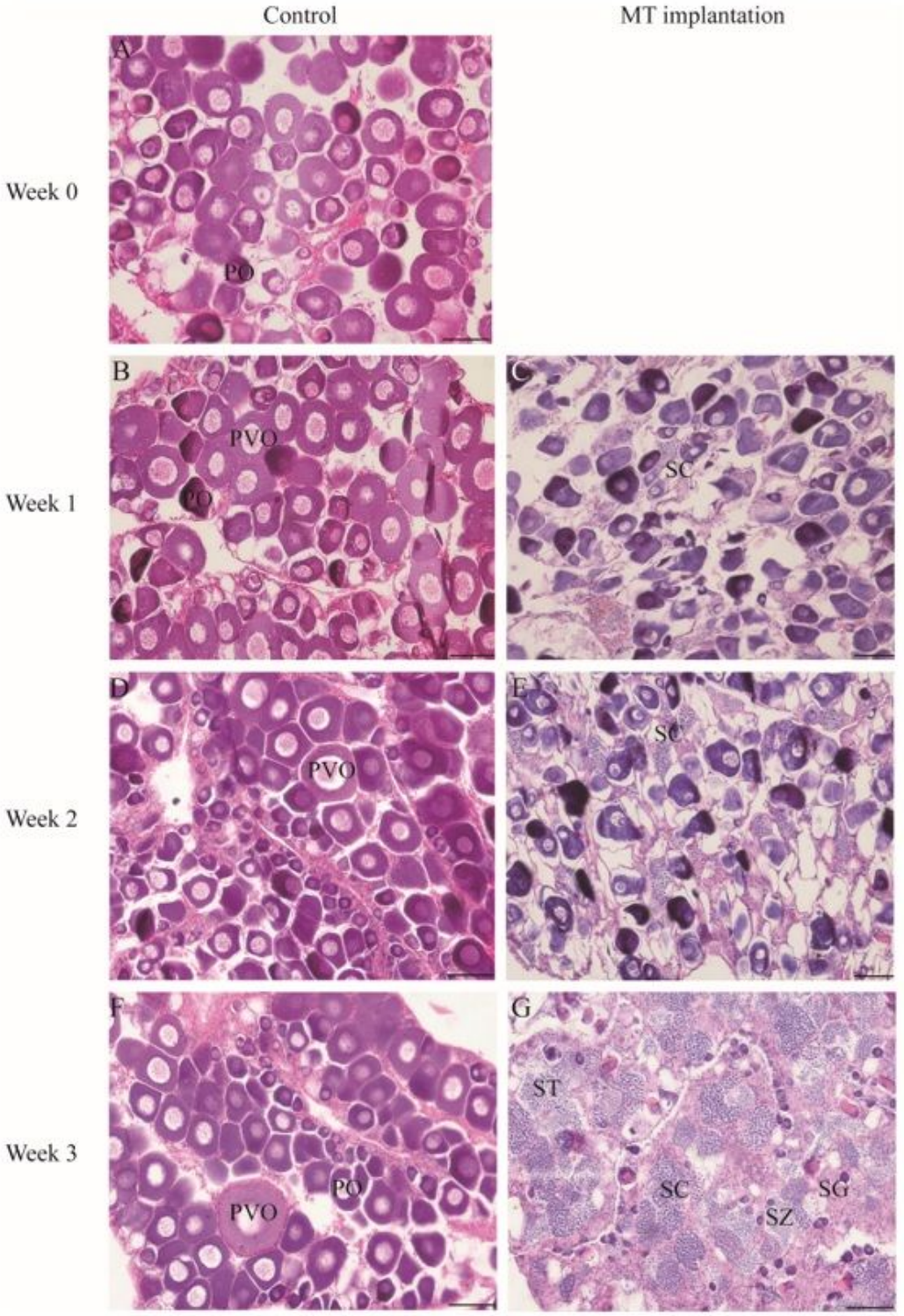

Figure 1

Figure 1

Histological effects of MT treatment on gonads of the orange-spotted grouper. (A, B, D and F) Histology of gonads in control fish. (C, E and G) Histology of gonads after MT implantation. PO, primary-growth stage oocyte; PVO, the cortical-alveolus stage oocyte; SG, spermatogonia; SC, spermatocyte; ST, spermatid; and SZ, spermatozoa. Scale bars = 50 um.

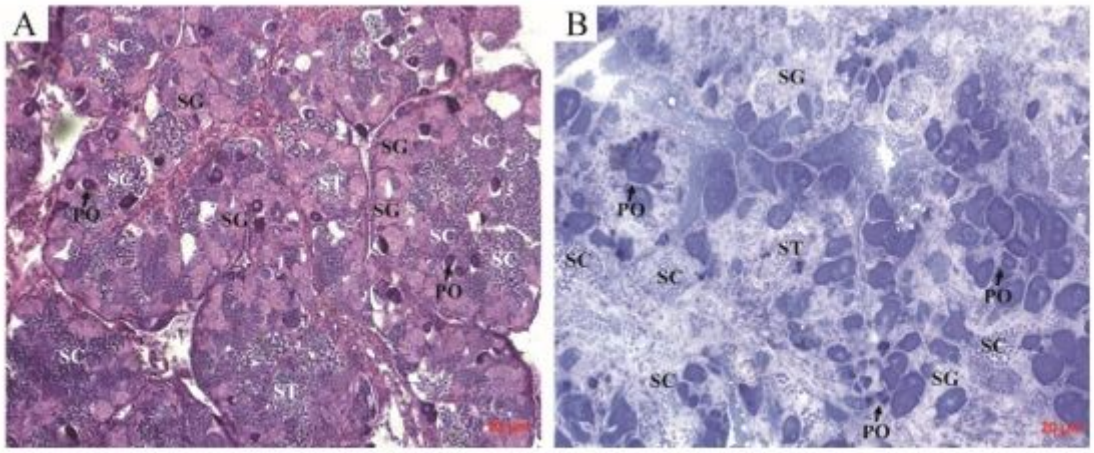

Figure 2

Figure 2

Gonadal structure by different staining methods. (A) Histological structure of gonad in MT treatment by H&E staining. (B) Histological structure of fresh gonad in MT treatment by cry-sectioning. SG, spermatogonia; SC, spermatocyte; ST, spermatid; SZ, spermatozoa; and PO, primary-growth stage oocyte. Scale bars = 20 um.

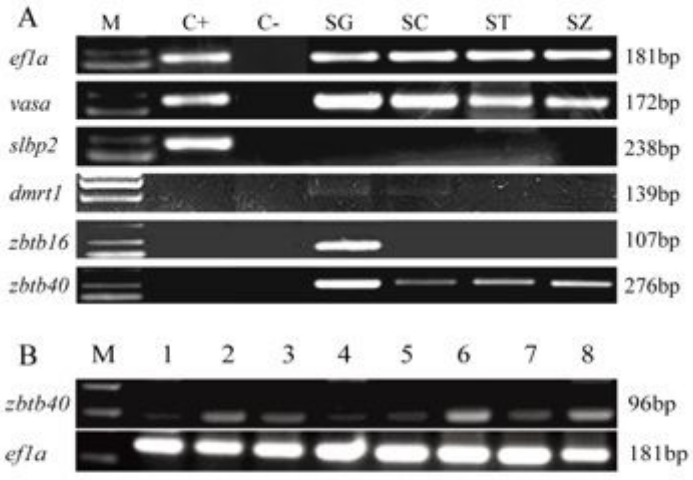

Figure 3

Figure 3

Expression of several sex-related genes and tissue distribution of Eczbtb40. (A) Expression of several sex-related genes in four cell types by laser capture. Ef1a was used as the reference gene. M, maker 2000; C+, the cDNA of ovaries (stayed at the stage with the portion of mostly PO) as a positive control; C-, template-

free as a negative control; SG, spermatogonia; SC, spermatocyte; ST, spermatid; SZ, spermatozoa. (B) Tissue distribution of Eczbtb40 in orange-spotted grouper. The ovaries of the fish stayed at the stage with the portion of mostly primary-growth stage oocytes (PO) and the testis from the mature male. Ef1a was used as the reference gene. M, maker 2000; 1, the whole brain; 2, heart; 3, head kidney; 4, liver; 5, kidney; 6, pituitary; 7, ovary; 8, testis.

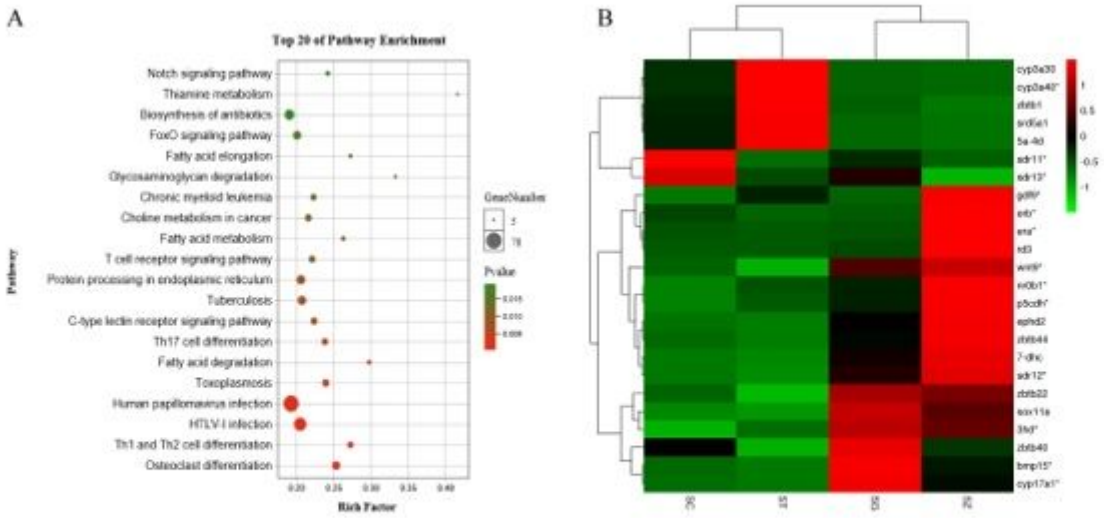

Figure 4

Figure 4

Analysis data of transcriptome. (A) The top 20 pathways in KEGG analysis with the significant difference. (B) A heat map was constructed based on the selected genes. Red indicated high expression and green low expression.

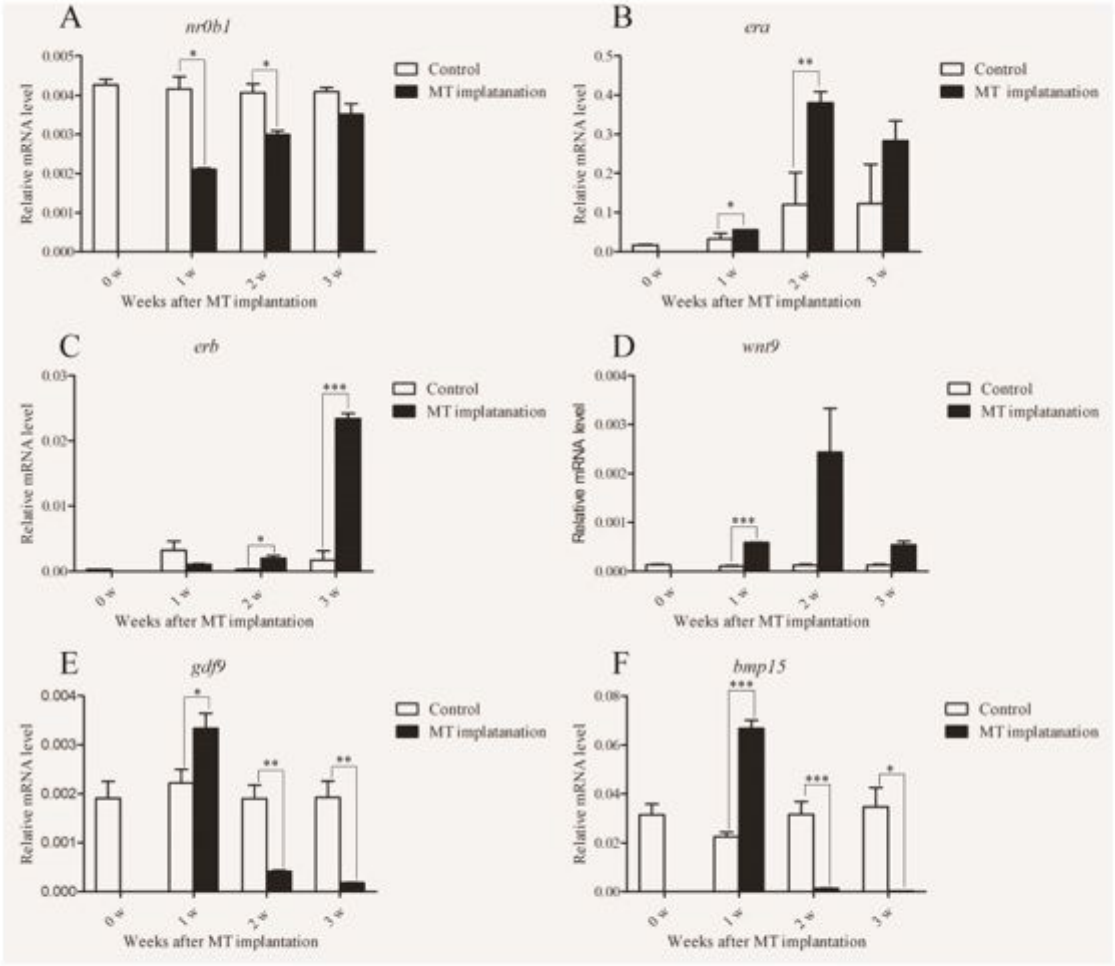

Figure 5

Figure 5

Validation of selected genes using RT-PCR. (A) nuclear receptor subfamily 0 group B member 1 (nr0b1); (B) estrogen receptor alpha (era); (C) estrogen receptor beta (erb); (D) protein Wnt-9 (wnt9); (E) growth and differentiation factor 9 (gdf9); (F) Bone morphogenetic protein 15 (bmp15).

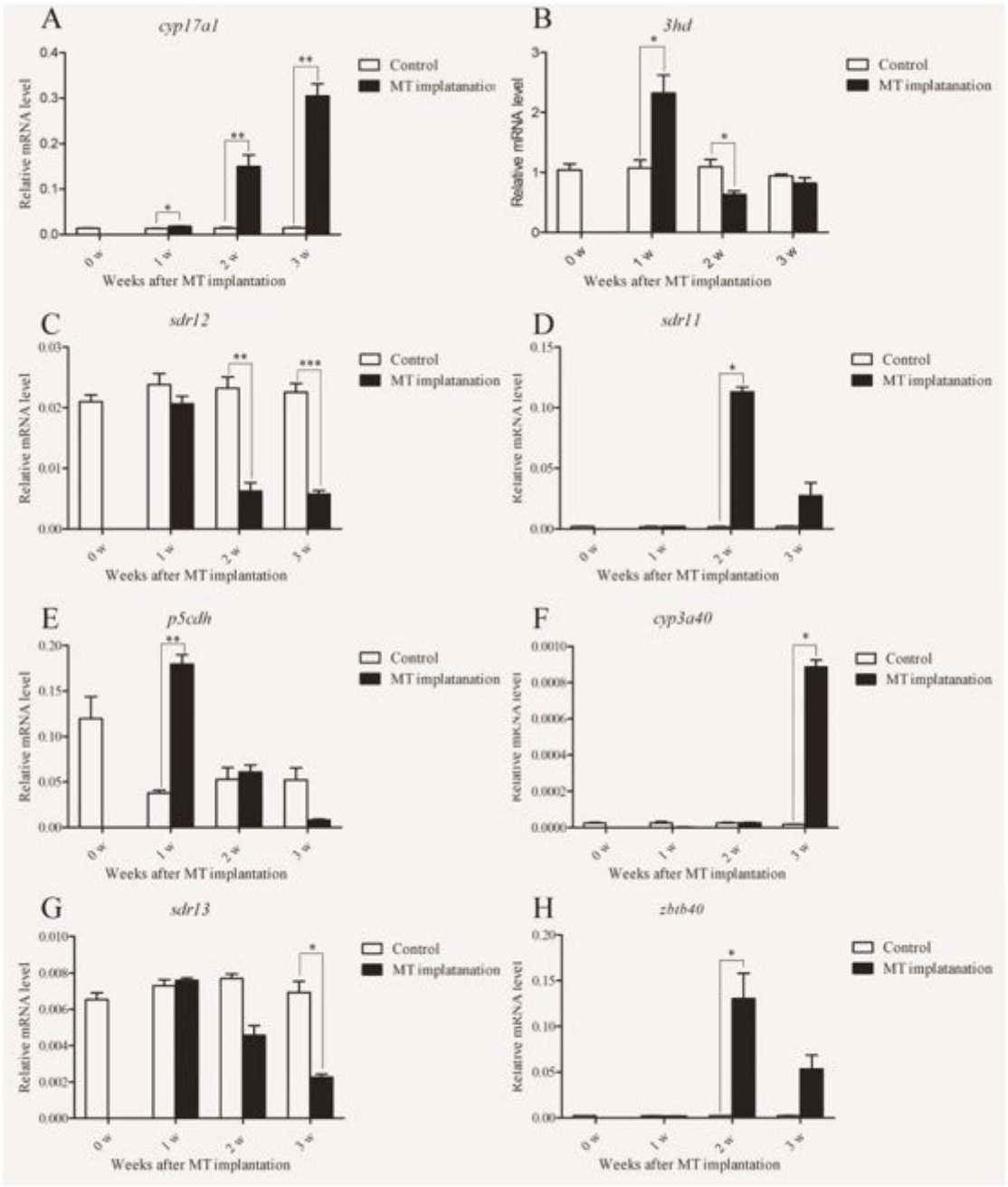

Figure 6

Figure 6

Validation of selected genes using RT-PCR. (A) Steroid 17-alpha-hydroxylase (cyp17a1); (B) 3-hydroxyisobutyrate dehydrogenase (3hd); (C) dehydrogenase/reductase (SDR) family member 12 (sdr12); (D) SDR family member 11 (sdr11); (E) delta-1-pyrroline-5-carboxylate dehydrogenase (p5cdh); (F) cytochrome P450 3A30-like (cyp3a30); (G) SDR family member 13 (sdr13); (H) zinc finger and BTB domain containing 16 (zbtb40).

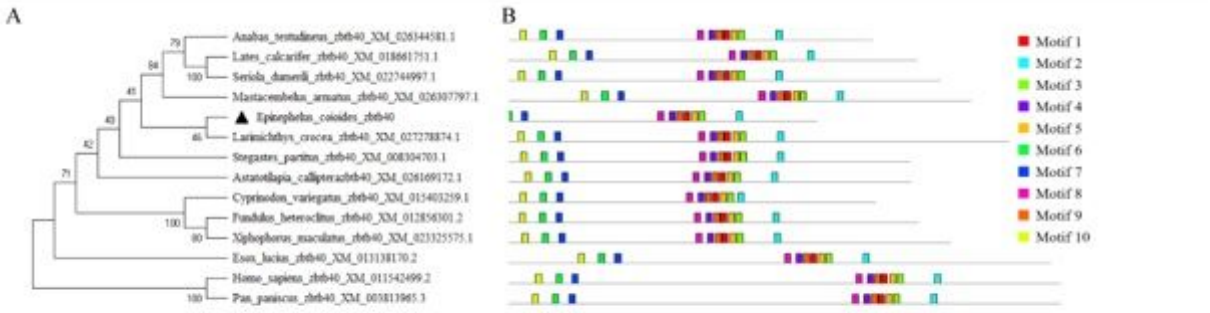

Figure 7

Figure 7

Phylogenetic relationships and conserved DNA motifs in zbtb40 genes from 14 species. (A) Phylogenetic tree of zbtb40s were conducted by MEGAX using the neighbor-joining likelihood method with 500 bootstrap replicates. Numerals at nodes were bootstrap values. The species names are followed by sequence accession numbers. (B) The top ten motif composition of zbtb40s. The motifs, numbers 1–10, are displayed in different colored boxes. The sequence information for each motif is provided in Supplementary table 1.

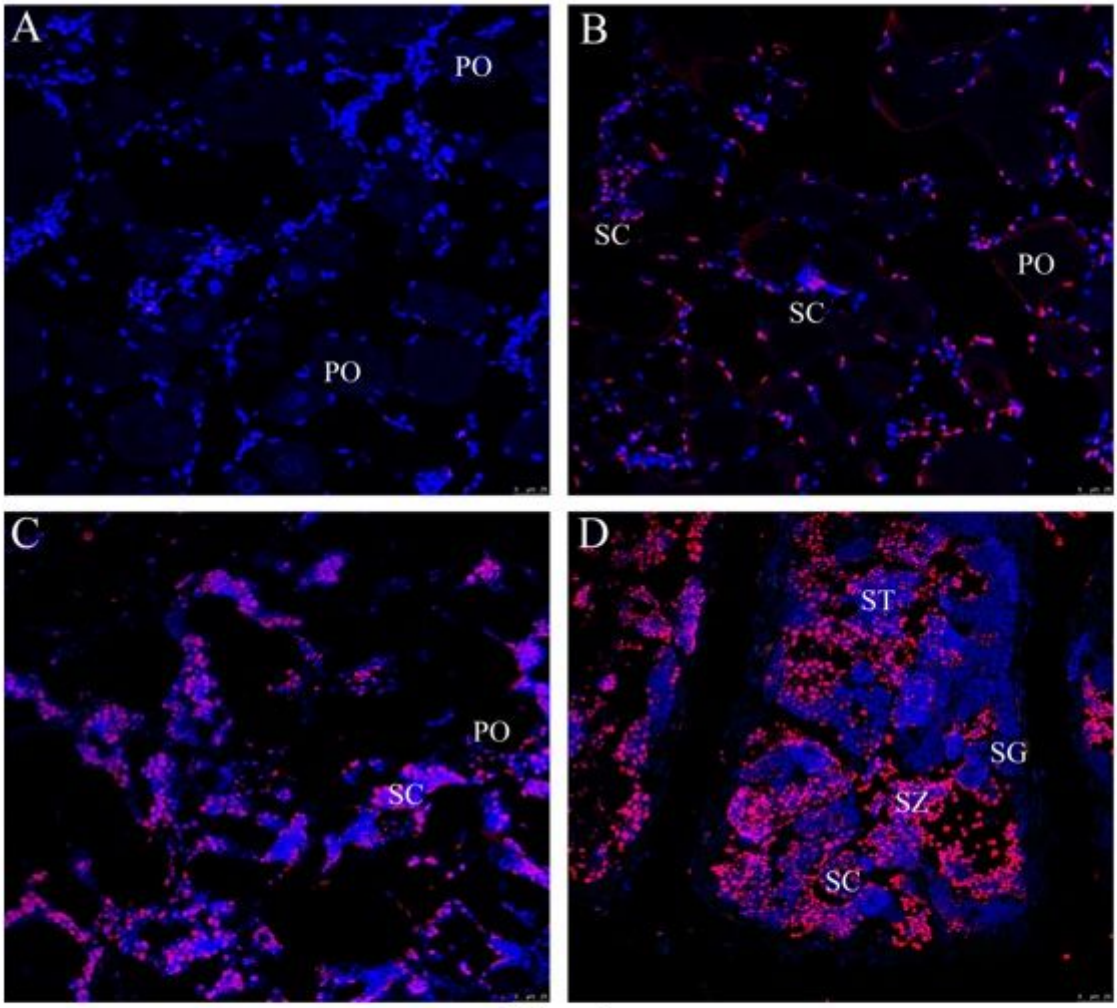

Figure 8

Figure 8

ISH analysis the Eczbtb40 mRNA expression in gonads at the sex reversal process by artificial MT implantation. (A) Gonadal stage with the portion of mostly primary-growth stage oocytes, (B) gonadal stage after one weeks of MT implantation, (C) gonadal stage after two weeks of MT implantation, (D) gonadal stage after three weeks of MT implantation. Red signals indicate Eczbtb40, blue staining indicates nuclei. PO, primary-growth stage oocyte; ST, spermatids; SZ, spermatozoa. Scale bars = 50 μm.

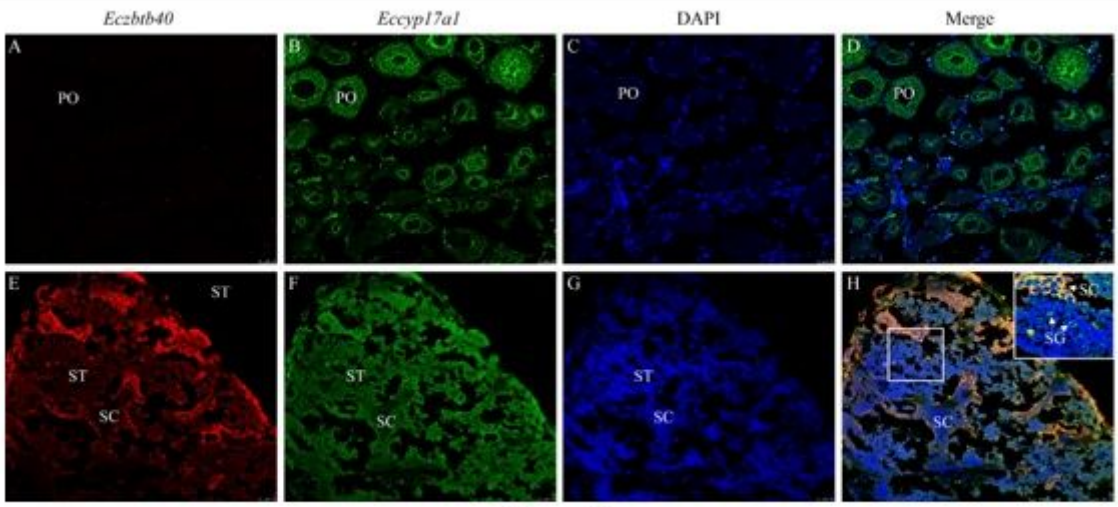

Figure 9

Figure 9

Co-localization of Eczbtb40 and Eccyp17a1 by FISH in the gonad of ovary (A-D) and testis (E-H). Gonad sections were stained red for Eczbtb40 mRNA, green for Eccyp17a1 mRNA and blue for DAPI. Red and green colors generated a yellow color. PO, primary-growth stage oocyte; SG, spermatogonia; SC, spermatocyte; ST, spermatid. Scale bars = 25 μm.

Supplementary Files

This is a list of supplementary files associated with this preprint. Click to download.

- supplement1.pdf
- supplement2.xlsx
- supplement3.pdf